Wärme- und Stoffübertragung 5 (1972) 31–38

Steady Turbulent Flow and Heat Transfer Downstream of a Sudden Enlargement in a Pipe of Circular Cross-Section

A. K.RUNCHAL, Kanpur, and D. B. SPALDING, London

Abstract. Stream-line and temperature contours, and the corresponding fluxes at the walls, are computed by numerical solution of the elliptic transport equations of vorticity, enthalpy and turbulence energy, together with auxiliary relations comprising a turbulence model similar to that of Prandtl [19]. The length-scale distribution is determined empirically in order to ensure that the recirculation region has the right length, and the maximum of the wall heat flux occurs at the right place, but the other empirical inputs have values which are determined from quite different experiments. – Agreement between predictions and experimental data of Krall and Sparrow [13] is good. In particular, the correct exponent is predicted for the Stanton number ∿ Reynolds number law. This exponent is uninfluenced by the length-scale distribution. – For practical use, it is argued, the Prandtl turbulence model needs to be replaced by one embodying two differential equations for turbulence quantities.

Zusammenfassung. Stromlinien und Isothermen und die entsprechenden Wärmeströme an der Wand werden berechnet durch Lösung der elliptischen Transportgleichungen für Wirbelausbreitung, Enthalpie und Turbulenzenergie zusammen mit Hilfsbeziehungen für ein Turbulenzmodell ähnlich dem von Prandtl [19]. – Die Verteilung des Längenmaßstabs erfolgt empirisch, um sicher zu gehen, daß der Rezirkulations-Bereich die richtige Länge besitzt und der maximale Wärmefluß an der richtigen Stelle der Wand auftritt. Andere empirische Vorgaben stammen von ganz unterschiedlichen Experimenten. – Die Übereinstimmung zwischen den berechneten Werten und den experimentellen von Krall und Sparrow [13] ist gut. Insbesondere konnte der genaue Exponent für das Stanton-Reynolds-Gesetz berechnet werden. – Für die praktische Anwendung wird empfohlen, das Prandtlsche Turbulenzmodell durch ein Modell zu ersetzen, das zwei Differentialgleichungen für turbulente Größen einschließt.

Nomenclature

C's	Constants
h	specific enthalpy
k	kinetic energy of turbulence
l	length scale of turbulence
p	static pressure
Pr	Prandtl number
q	heat flux
r	radius
R	radius of pipe
Re	Reynolds number
s	skin-friction coefficient
St	Stanton number
u	axial velocity
y	distance from the pipe wall
z	axial distance from the point of enlargement
Z	non-dimensional axial distance
Γ	coefficient of diffusional transport
ϵ	dissipation of k
μ	viscosity
ρ	density
σ	Prandtl number
τ	shear stress
ϕ	general dependent variable
ψ	stream-function
ω	vorticity

Subscripts

e	effective value
F	value in the field
h	pertaining to h
k	pertaining to k
m	mean value
S	value at the wall
ϵ	pertaining to ϵ
μ	pertaining to μ

1. Introduction

1.1. The Problem under Consideration

Downstream of the sudden enlargement of diameter of a pipe, or in the wake of a bluff body, there often occurs a turbulent recirculating flow. In some ranges of geometrical shape and Reynolds number regular pulsations are found; these may be associated with 'vortex-shedding'. More frequently, however, the fluctuating motion appears to be an entirely random one, superimposed on a time-average flow with a clearly discernible continuity of existence; it is this situation that is here in question.

* Dedicated to Prof. Dr.-Ing. U. Grigull on his 60th birthday.

Engineers have long been forced to observe the quantitative effect of such turbulent 'separated' flow; for the recirculation phenomenon may account for a large portion of the power that is needed to pump the fluid; the heat-transfer rates to walls confining the flows are often exceptionally large; and sometimes a recirculation is deliberately introduced so as to anchor a flame in a high-velocity stream of combustible gas.

Theoreticians have been rather less eager to give recirculating flows their attention; for boundary-layer theory is inapplicable to them, and so the elliptic nature of the governing equations has been a deterrent. Moreover, there have been puzzling regularities in the phenomena that have defied explanation. One of these is that the Stanton number has varied in proportion to the Reynolds number to a characteristic power, about -0.35; this lies obstinately between the -0.20 which characterises many other turbulent flows and the -0.50 which is exhibited by laminar flows.

An explanation of the Reynolds-number exponent was proposed by one of the present authors [23], who argued that the special feature of heat transfer from separated flow is that the turbulent motions adjacent to the surface are not produced by the local shear stresses, but by those which exist at a quite different location in the flow field; the turbulence energy is transported from the generation area to the surface by convection and diffusion; and the ratio of certain constants describing dissipation and diffusion plays a big part in determining the exponent.

The main defect of the afore-mentioned contribution was that it rested on an equation for the transport of turbulence in one dimension; whereas the flow behind a bluff body is of course two-dimensional. Consequently, although the Reynolds-number exponent could be quantitatively determined, the actual values of Stanton numbers were estimated only as to order of magnitude. At the time, no procedure was readily available for solving the two-dimensional equations; and indeed no solutions appear to have been published since that date.

The present paper therefore takes the matter a step forward, by applying to the same model of turbulence a solution procedure which has recently been published, for more general problems, by the authors and their colleagues [7]. A particular separated flow is selected, namely that provoked by an abrupt enlargement in a pipe of circular cross-section. Predictions are made of the distributions of velocity, turbulence energy and other properties within the fluid, and of shear stress and heat-transfer coefficient along the wall. The former are found to be plausible and of the correct order of magnitude, though experimental data are not available for comparison; the Stanton-number predictions are however compared with experiment, and with good success.

1.2. Method of Attack

The turbulence model

The essential idea of the earlier paper, by Spalding [23], was a distillation of those which had appeared in the works of Prandtl [19], Emmons [4], Townsend [24] and Glushko [6]: the state of the turbulence at any point is characterised by two measures, the energy and a length scale; and the former is governed by a differential equation, while the latter is a simple function of the distance from the wall. A similar idea, differently elaborated, has been employed by Bradshaw and co-workers in a number of recent papers concerned with boundary-layer flows (e.g. Ref. [2]).

In recent years, several models of turbulence have come into prominence which entail the solution of differential equations not only for the turbulence energy, but also for one or more additional quantities. Thus Kolmogorov [12] proposed an equation for the 'turbulence frequency'; the length scale was to be determined by dividing the square root of the energy by this quantity. Rotta [20] provided equations for the product of energy and length, and for the turbulent shear stress. Spalding and co-workers (see, e.g., Ref. [15]) have concentrated attention on models having energy as the first dependent variable and various combinations of energy and length as the second. The Los Alamos group (see, e.g., Ref. [9]) have worked with two-, three-, and five-equation models.

The work to be reported in the present paper was begun before the developments of the last paragraph had attracted attention. It is therefore based upon the one-differential-equation model which underlay the one-dimensional treatment of separated-flow heat transfer. Restriction of attention to this simple model has three advantages: (i) The step from one dimension to two is already large enough; to change the turbulence model at the same time would obscure the effects of the changed dimensionality. (ii) The multi-equation models are still in a state of competitive development; by using none, we escape the necessity for a premature selection. (iii) The use of a one-equation model for a separated flow, and the exposure of its inadequacies, makes the case for developing a two-equation model, which some have questioned [1], extremely clear. Provided that the limitations of the model are recognised, therefore, valuable lessons can be learned from its application to separated flows.

The computational procedure

The only practicable way of calculating turbulent-flow phenomena at the present time is to treat the fluid as though it were a laminar non-Newtonian one: the differential equations for the time-mean velocity, vorticity, etc., are therefore the same as for laminar flow, but the shear stresses are non-linearly related to the shear strains. These equations can be solved, with general boundary conditions, only by numerical means; they must first be converted into their finite-difference equivalents; then an iterative numerical procedure must be devised which converges at length to their solution.

More than one such procedure has been reported for two-dimensional flows (e.g. Ref. [3, 5, 8, 22]), but many of these fail to converge at high Reynolds numbers; and few have been used for other than constant-viscosity fluids. Building upon the foundation of the last-named reference, the authors and their colleagues have recently developed a fairly general method of solving the equations. This is convergent even at high Reynolds numbers; it is capable of handling non-uniform viscosities; and it can solve the equations of heat and turbulence energy transport at the same time as those for the hydrodynamic quantities. This is therefore the method that has been used in the present work. Because full details are reported in the book by the authors and their colleagues [7], which also contains a listing of a general computer programme, it should be sufficient here to present merely the differential equations, the boundary conditions, and the results of the computations.

1.3. The Geometry Selected

Fig. 1 shows schematically the configuration of the pipe for which the computations have been performed. An incompressible fluid flows from the small-diameter pipe on the left into a second pipe of double the diameter. Downstream of the join there exists a region of reverse flow, about two diameters long; this is followed by a region of redeveloping flow in which the fluid gradually assumes the self-similar behaviour which is characteristic of flow in a long straight pipe.

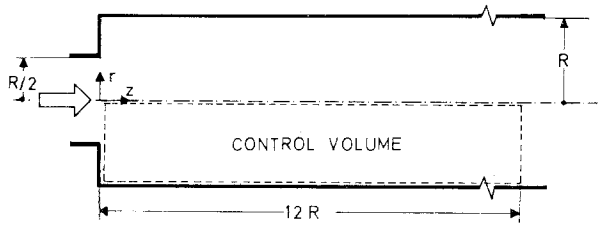

Fig. 1. The geometry of the problem

The Reynolds number is supposed to be high enough for the fluid to be turbulent everywhere except in the immediate vicinity of the pipe walls.

This geometry has been selected because there exist some published experimental data [13] for the heat transfer to the wall of a circular-section pipe in which is inserted an axi-symmetrical constriction; the central aperture of this has half the diameter of the pipe. This geometry, it may be considered, is near enough to that of Fig. 1 for comparisons between the predictions and the experimental data to be informative.

The fluid crossing the enlargement section has a uniform velocity and temperature. The wall of the down-stream section has a temperature distribution consistent with uniformity of heat-flux per unit area. Our main task is to calculate the distribution of dimensionless heat-transfer coefficient (Stanton number) along this wall. We shall be interested in the way the Stanton number depends upon the Reynolds number; but we shall hope, this time, to predict the absolute values of the Stanton number correctly, and not merely the Reynolds-number exponent.

Of course, in order to calculate the heat-transfer coefficients to the wall, we have to solve the hydrodynamic equations also. We shall therefore be making predictions of the distributions of velocity, stream-function, vorticity and turbulence energy throughout the volume of the pipe. Although there appear to be no experimental data which would allow these predictions to be verified, some representative predictions will be presented below, for the sake of the light which they throw on the probable mechanisms of the flow.

2. Analysis

2.1. Equations and Boundary Conditions

Differential equations

Four simultaneous elliptic differential equations govern the process; their dependent variables are the specific enthalpy h, the turbulence energy k, the stream-function ψ, and the vorticity ω. The equations can be expressed in a common form:

$$a\left\{\frac{\partial}{\partial z}\left(\phi\frac{\partial\psi}{\partial r}\right)-\frac{\partial}{\partial r}\left(\phi\frac{\partial\psi}{\partial z}\right)\right\}=\frac{\partial}{\partial z}\left\{b\frac{\partial}{\partial z}(c\phi)\right\}+\frac{\partial}{\partial r}\left\{b\frac{\partial}{\partial r}(c\phi)\right\}+d\,, \tag{2.1}$$

where ϕ stands for any one of h, k, ψ and ω, where r and z are respectively radial and the axial distance co-ordinate, and where the symbols a, b, c and d stand for the expressions that are assembled in the following table.

Table 1. Expressions appearing in Eq. (2.1)

ϕ	a	b	c	d
h	1	$\Gamma_{e,h}$	1	0
k	1	$\Gamma_{e,k}$	1	rS
ψ	0	$(\rho r)^{-1}$	1	ω
ω/r	r^2	r^3	μ_e	0

The term S appearing in the above table is given by:

$$S = \frac{\mu_e}{\rho^2}\left\{2\left[\frac{\partial}{\partial z}\left(\frac{1}{r}\frac{\partial \psi}{\partial r}\right)\right]^2 + 2\left[\frac{\partial}{\partial r}\left(\frac{1}{r}\frac{\partial \psi}{\partial z}\right)\right]^2 + \left[\frac{\partial}{\partial r}\left(\frac{1}{r}\frac{\partial \psi}{\partial r}\right) - \frac{\partial}{\partial z}\left(\frac{1}{r}\frac{\partial \psi}{\partial z}\right)\right]^2\right\} - \rho\epsilon \tag{2.2}$$

Various symbols appearing in this equation and the above table are explained in the nomenclature at the front of the paper. This table is a simplified version of the one appearing in the book previously referred to [7]. The simplifications arise from our restriction of consideration to uniformity of fluid density, to low velocities, and to the absence of swirl about the axis. The d-term of the vorticity equation has been shorn of certain small terms involving effective-viscosity gradients; the motive is to reduce computational labour, and the justification is that to account for turbulent-vorticity transport by way of an isotropic effective viscosity is at best a plausible first approximation.

Auxiliary algebraic equations

The differential equations contain the diffusional transport properties of vorticity, turbulence energy and enthalpy, namely, μ_e, $\Gamma_{e,k}$ and $\Gamma_{e,h}$. Our chosen turbulence model allows us to express these quantities in terms of the turbulence energy k and its length scale l by way of:

$$\mu_e = C_\mu \rho k^{1/2} l , \tag{2.3}$$

$$\Gamma_{e,k} = \mu_e/\sigma_{e,k} , \tag{2.4}$$

$$\Gamma_{e,h} = \mu_e/\sigma_{e,h} . \tag{2.5}$$

Here C_μ, $\sigma_{e,k}$ and $\sigma_{e,h}$ are the supposedly universal constants; their values will be discussed in Section 2.2.

Our model of turbulence allows the rate of dissipation of energy, ϵ, to be determined from the equation

$$\epsilon = C_\epsilon k^{3/2}/l . \tag{2.6}$$

Eqs. (2.3) to (2.6) can be expected to hold only in regions in with the local Reynolds number of turbulence ($\equiv \rho k^{1/2} l/\mu$, where μ is the molecular viscosity) is very large. This condition is certainly not satisfied in the neighborhood of the walls; so special practices are needed to account for the viscous effects which prevail there. Our practice is a development of that adopted in the earlier paper [23]: the above equations are presumed to apply in all but a thin region close to the wall, the inner edge of which is characterised by a definite value of the local Reynolds number of turbulence. Within this layer, the fluid is taken to be laminar; and the fluxes of momentum, heat and turbulence energy across it are taken to obey laws whose forms are derived from experimental data for especially simple circumstances.

The particular relations which have been used are:

$$\tau_S = u_F(1 - I_2)/I_1 , \tag{2.7}$$

$$q_S = (h_F - h_S)/I_3 . \tag{2.8}$$

The I's are given by:

$$I_1 = \int_0^{Y_F} u_e^{-1}\, dy , \tag{2.9}$$

$$I_2 = \left(u^{-1}\frac{d\rho}{dz}\right)_F \int_0^{Y_F} \mu_e^{-1} y\, dy , \tag{2.10}$$

$$I_3 = \int_0^{Y_F} \sigma_{e,h}\mu_e^{-1}\, dy . \tag{2.11}$$

These integrals can be evaluated with proper assumptions for the variations of μ_e and $\sigma_{e,h}$. A detailed analysis is given in Runchal [21].

Boundary conditions

The domain over which the equations are to be integrated is that enclosed within the control surface shown in Fig. 1. At the inlet section, the fluid is taken to have uniform velocity, the stream-function is therefore quadratic in radius, and the vorticity is zero. The enthalpy is given an arbitrary uniform value, and so is the turbulence energy; the first of these ascriptions has no influence on the calculations, but the second does so; however its influence was found to be very weak [21], and finally the turbulence energy of the incoming fluid was fixed at 3%.

At all walls, the stream-function was prescribed, and the vorticity was chosen so as to satisfy the no-slip condition. The turbulence energy was zero, and the enthalpy was specified by way of a heat-flux prescription. The step-wall was always taken as adiabatic.

Because the equations are elliptic, the mathematical problem is not complete unless sufficient information is supplied about conditions at the whole of the boundary. It is therefore necessary to supply boundary

conditions for the exit plane, even though, strictly speaking, we do not know what state the fluid will be in when it emerges from the domain of integration. Fortunately, as will be readily believed by those who possess experimental knowledge of flows of this type, the effects of the exit boundary conditions are significant for only a short distance upstream, say one pipe diameter. Therefore, provided that the region of interest is a few diameters upstream of the exit section, it matters very little what conditions are supplied at the exit section. We have accordingly set our exit section at six large-pipe diameter from the inlet, and all the variables were constrained to have zero gradients in the axial direction at the exit section.

The boundary conditions at the axis of symmetry were those of the vanishing gradients in the radial direction.

2.2. Physical Inputs

The length-scale distribution

The quantity l, which appears in Eqs. (2.3) and (2.6) must be ascribed a value at every point of the field. In the earlier paper [23], it was sufficient to suppose that l was proportional to the distance from the wall, just as Prandtl had done; inside a duct however, some account must be taken of the fact that the distance from any point to the wall depends on the direction of travel; and one must expect also that the flow pattern itself influences the l-distribution.

A comparison of predictions obtained by using various empirically-assumed l-distributions is given by Runchal [21]. The length-scale distribution finally used for the computations of section 3 was that given by taking l as the smallest of the following:

$$l = C_1^{-1} \exp\,[C_1(R - r) - 1]\,, \tag{2.12}$$

$$l = C_2 R (Z/R)^{C_3}$$

$$l = C_4 R\,, \tag{2.14}$$

where C's are numerical constants. Many sets of values for these constants were tried; the values found most satisfactory were 60, 0.08, 1.09 and 0.6 respectively. The requirements for acceptance were, firstly, that the reattachment should be caused between six and eight step-heights from enlargement and, secondly, that heat-transfer maxima should appear in the immediate vicinity of the reattachment point. These criteria stem from experimental evidence.

It should be pointed out that Eq. (2.12) ensures that for regions close to a wall, i.e. where r approaches R, l tends to a value equal to the distance from the wall. The second equation expresses the fact that as the shear-layer grows, starting from the point of separation, the length scale also grows. In an unconfined shear layer the rate of growth will be linear, however it was found that a better agreement with experimental data could be obtained by using a slightly faster growth rate. Eqs. (2.12) and (2.13) cannot be used for large Z or R as they give unrealistically large values for l; therefore, Eq. (2.14) was used to limit the maximum value of l.

Values of the constants

In section 2.1, a number of supposedly universal constants were introduced. Their values were presumed to be: $C_\mu = 0.20$, $C_\epsilon = 0.31$, $\sigma_{e,k} = 1.5$, and $\sigma_{e,h} = 0.5$. These values are close to those derived from experimental data and employed by Spalding [23] in the earlier study.

2.3. Tests of Mathematical Accuracy

Finite-difference solutions are known to be subject to truncation errors, of which the magnitudes depend on the grid size. The accuracy of a finite-difference solution must therefore be checked by using different grid sizes for a test case.

The Stanton number and the wall shear stress for three different grids are shown in Fig. 2. (From Ref. [21]). The results for a 21 x 15 grid (21 nodes in the axial direction and 15 in the radial direction) are in good agreement with those for the grids of 32 x 15 and 32 x 22. It can therefore be concluded that the 21 x 15 grid, which was used for all the computations to be reported below, was fine enough to give sufficient mathematical accuracy.

3. Results and Discussion

3.1. The Predictions

The non-dimensional parameters

For convenience of interpretation, we define the following nondimensional parameters:

non-dimensional distance: $Z \equiv 2z/R$,
skin-friction coefficient: $s \equiv \tau_S/\rho\, u_m^2$,
Reynolds number: $Re \equiv 2\rho\, u_m R/\mu$,
Prandtl number: $Pr \equiv \mu/\Gamma_h$,
Stanton number: $St \equiv q_S/[\rho u_m (h_m - h_S)]$.

The mean enthalpy h_m was assumed to vary linearly between the inlet and the outlet sections; as the values of h_m varied by only 1% between the two sections, this assumption is not likely to cause any significant error in calculations.

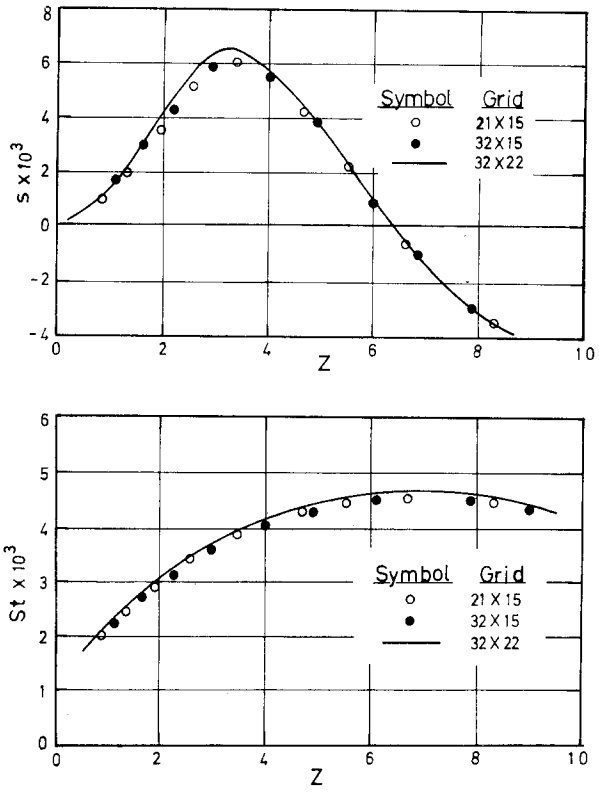

Fig. 2. The influence of grid-size

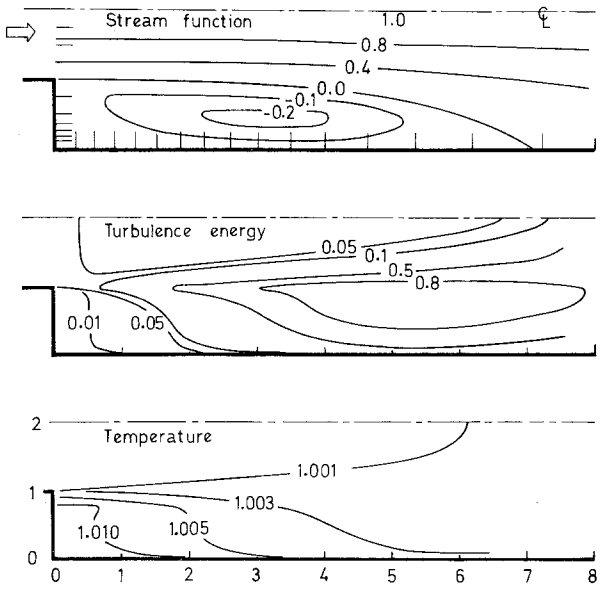

Fig. 3. Flow patterns in the sudden enlargement; Re = 50 000, Pr = 3

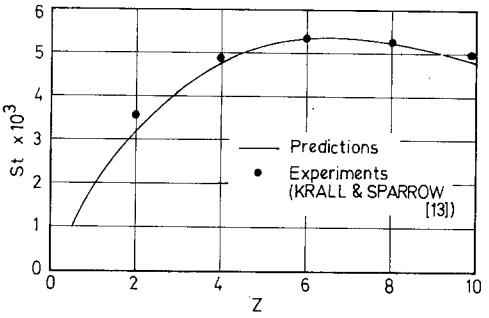

Fig. 4. Computed and experimental Stanton number downstream of enlargement; Re = 51 500, Pr = 3

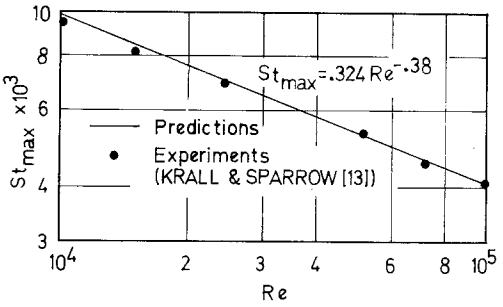

Fig. 5. Computed and experimental Stanton number maxima at the reattachment point

quantity has been non-dimensionalised in terms of the pipe-radius R and the mean velocity u_m. The locations of the grid lines are shown in the top diagram. The downstream part of the grid, beyond 8 step-heights has been omitted from the diagrams as it does not contain any significant information.

The stream-function contours show the formation of a closed eddy, extending a distance of seven step-heights downstream of enlargement. This fact is in accordance with empirical observations.

The contours of turbulence energy reveal the formation of a high shear region starting from the point of separation. The maximum turbulence level ($k/(16\,u_m^2) \approx 0.05$) compares well with the available measurements in similar situation, such as the flow of a uniform-velocity stream past a step [16].

The temperature contours reveal that, apart from a thin region close to the pipe wall and a part of the eddy, the whole of the fluid is virtually at the temperature of the incoming jet. This is an understandable consequence of the high Reynolds number and the intense mixing in the high-shear region.

Qualitative description of the predictions

Fig. 3 presents the contours of stream-function, turbulence energy and temperature for a Reynolds number of 50.000 and Prandtl number of 3. Each

Comparison between theory and experiment

Figs. 4 and 5 compare the computed Stanton number distribution with the experimentally observed values of Krall and Sparrow [13].

Both the St $\sim$ Z dependence of Fig. 4 and the St $\sim$ Re dependence of Fig. 5 are predicted correctly. The agreement in respect of the Reynolds number exponent, -0.38, is especially gratifying because, as mentioned above, this value is unlike those of more commonly analysed flows.

3.2. The Adequacy of the Turbulence Model

The agreement between the predictions and the experimental data is of course to be attributed in part to the proper choice of values for the constants C_μ, C_ϵ, $\sigma_{e,k}$ and $\sigma_{e,h}$. However, these values have not been chosen primarily by reference to the experiments which we are here considering; they accord well with experimental data of quite different types. For example, it is easy to show that, in a region of uniform shear stress near a wall, the ratio of shear stress divided by turbulence energy times density is given by:

$$\tau/\rho k = (C_\mu\, C_\epsilon)^{1/2} \qquad (3.1)$$

With the constants chosen, this ratio has the value of 0.25, which is close to the value of 0.28 reported by Laufer [14] and that of 0.30 reported by Klebanoff [11].

Had it been necessary to employ very different values of the constants, in order to produce good predictions of separated flows, the credibility of the turbulence model would have been seriously impaired. However, the model has passed this test quite well.

The main defect of the model, which it shares with the two other extant one-equation models, namely those of Bradshaw et al. [2] and of Nee and Kovasnay [17], is its need for a complete specification of the distribution of the length scale within the flow space. For boundary-layer flows on walls, this necessity is not so troublesome as to preclude the models from practical employment; for it appears that the length-scale distribution across the layer can be expressed as a nearly universal function of position within the layer; this function is indeed not very different from that which earlier workers (see e.g. Ref. [10]) found to characterise the mixing length of Prandtl's [18] hypothesis.

For separated flows, with their large variety of boundary shapes and fluid-entry conditions, no rules exist which would allow the length-scale distribution to be prescribed in advance. Thus, the prescription of Eqs. (2.12) to (2.14) was arrived at only after extensive trials of alternatives, guided by comparison of the resulting predictions with the experimental data. While all the length-scale distributions led to substantially the same Reynolds-number dependence of the Stanton number, the location and magnitude of the maximum of St were markedly influenced by the choices made for l. Consequently although the present investigation has shown that a one-equation turbulence model can be contrived which fits the experimental data for separated flows, engineering designers will obtain much better guidance from models possessing two differential equations for statistical properties of turbulence; for from these models, of which Kolmogorov's [12] was the first, the length-scale distributions can be predicted.

4. Conclusions

(a) It has proved possible to explain the salient features of fluid flow by the application of a model of turbulence which accounts for the generation, dissipation, convection and diffusion of the kinetic energy of the fluctuating motion. The constants in the equation are close in magnitude to those found applicable to boundary-layer flows.

(b) The Stanton number has been correctly predicted to vary as the -0.38 power of the Reynolds number.

(c) To produce agreement with the absolute values of the Stanton number, a particular length-scale distribution had to be devised. Because no general rules exist for prescribing such distributions, one-equation turbulence models of the present type have little predictive value for separated flows. They require to be superseded by models employing at least two differential equations for turbulence quantities; for from these the length-scale magnitude can be deduced at each point.

References

1. Bradshaw, P.: Proc. Boeing Sci. Res. Lab.'s Symposium on Turbulence, Seattle, Washington, 1969.
2. Bradshaw, P., Ferriss, D. H., Atwell, N. P.: J. Fluid Mech., 28 (1967) 593.
3. Burggraf, O. R.: J. Fluid Mech., 24, 1 (1966) 113/151.
4. Emmons, H. W.: Proc. 2nd U.S. Cong. Appl. Mech. A.S.M.E., 1, 1954.
5. Fromm, J. E., Harlow, F. H.: Physics of Fluids, 6, 7 (1963) 975/982.
6. Glushko, G. S.: Izv. Akad. Nauk S.S.S.R., Mekh. No. 4 (1965) 13.
7. Gosman, A. D., Pun, W. M., Runchal, A. K., Spalding, D. B., Wolfshtein, M.: Academic Press (London) 1969.
8. Greenspan, D.: Univ. of Wisconsin, Tech. Rep. No. 9 of the Dept. of Computer Sci., 1967.
9. Harlow, F. H., Daly, B. J.: Los Alamos Sci. Lab. Univ. California Rep. LA-DC-11304, 1970.
10. Hudimoto, B.: Kyoto Univ. Memoirs of Fac. of Eng., XIII, No. 4, 1951.
11. Klebanoff, P. S.: NACA TN3178, 1954.
12. Kolmogorov, A. N.: (In Russian) Izv. Akad. Nauk S.S.S.R. ser. Phys. No. 1–2, 1942.
13. Krall, K. M., Sparrow, E. M.: A.S.M.E., J. Heat Transfer, 88, 1 (1966) 131/136.

14. Laufer, J.: NACA Rep. 1174, 1954.
15. Launder, B. E., Spalding, D. B.: Proc. Sym. on Internal Flows, Univ. of Salford, 1971.
16. Mueller, T. J., Robertson, J. M.: Proc. 1st Southeastern Conf. on Theo. and Appl. Mech., Gatlinburgh, Tenn., May 3–4, 1962.
17. Nee, V. W., Kovasnay, L. S. G.: Conf. on Computation of Turbulent Boundary layers, Vol. 1, Stanford Univ., 1968.
18. Prandtl, L.: ZAMM 5 (1925) 136.
19. Prandtl, L.: Nachr. Akad. Wiss., Göttingen, IIA (1945) 6/19.
20. Rotta, J.: Z. für Physik 131 (1951) 51/77.
21. Runchal, A. K.: Ph. D. thesis, London University, 1969.
22. Runchal, A. K., Wolfshtein, M.: Imperial College, Mech. Eng. Dept., SF/TN/1, 1966.
23. Spalding, D. B.: J. Fluid Mech. 27, 1 (1967) 97/109.
24. Townsend, A. A.: J. Fluid Mech. 11 (1961) 97.

Dr. A. K. Runchal
Mechanical Engineering Department
Indian Institute of Technology
Kanpur, U. P. India

Professor D. B. Spalding
Mechanical Engineering Department
Imperial College
Exhibition Road
London SW 7 2BX, England

Received August 2, 1971